Brazilian Journal of Geophysics (2021) 39(1): 85–91

ISSN 0102-261X
DOI 10.22564/rbgf.v38i3.2078

# ANALYSIS OF MAGNETIC FIELD COMPONENTS ANOMALIES DUE TO HOMOGENEOUS POLYHEDRONS

Eduardo M. S. Amarante and Edson E. S. Sampaio

**ABSTRACT.** A procedure for determining semi-analytical expressions for the magnetic fields caused by homogeneous polyhedral bodies based on Green's theorem has been developed. It constitutes a modification of previous developments for the gravity field of three-dimensional bodies and employs the discretization of the faces of the polyhedron by triangles and the definition of local coordinates for each triangle. A maximum misfit of less than 1.0% between the values computed with these analytical expressions and those obtained with closed expressions for prismatic bodies, applied to a homogeneous cube, demonstrates the effectiveness of the procedure. Examples of magnetic maps due to octahedral bodies with different forms and orientations show that it is possible to obtain a qualitative distinction among their anomalies. Therefore, the present analysis constitutes a basis for future inverse modeling of convex polyhedrons and will be useful in geophysical exploration.

**Keywords:** magnetic anomalies, polyhedral bodies, irregular shapes.

**RESUMO.** Foi desenvolvido um procedimento para determinar expressões analíticas para os campos magnéticos causados por corpos poliédricos homogêneos com base no teorema de Green. Constitui uma modificação dos desenvolvimentos anteriores para o campo gravitacional de corpos tridimensionais e emprega a discretização das faces do poliedro por triângulos e a definição das coordenadas locais para cada triângulo. Um erro máximo inferior a 1,0% entre os valores calculados com essas expressões analíticas e os obtidos com expressões fechadas para corpos prismáticos, aplicados a um cubo homogêneo, demonstra a eficácia do procedimento. Exemplos de mapas magnéticos devido a corpos octaédricos com diferentes formas e orientações mostram que é possível obter uma distinção qualitativa entre suas anomalias. Portanto, a presente análise constitui uma base para futura modelagem inversa de poliedros convexos e será útil na exploração geofísica.

**Palavras-chave:** anomalias magnéticas, corpos poliédricos, formas irregulares.

Corresponding author: Eduardo M. S. Amarante

Universidade Federal da Bahia - UFBA, Instituto de Geociências, Campus Universitário de Ondina, Salvador, BA, Brazil, 40170-290 - E-mails: edu.amarante18@gmail.com, starteri@ufba.br

## INTRODUCTION

The literature of analytical solutions for gravimetric and magnetic fields at observation points external to bodies with polyhedral geometry is extensive. Cady (1980) computed gravity and magnetic anomalies along a single profile for a polygonal prism with a constant cross section, known as 2.5D model. Werner (1994) and Werner and Scheeres (1996) have derived closed expressions for the gravity potential due to a homogeneous polyhedron solving the surface integral as a function of the solid angle and summing line integrals along polygonal contours. Götze and Lahmeyer (1988) determined an analytical expression of the gravity field of a polyhedral body as a function of its edges by transforming the volume integral into a sum of line integrals and modeled the respective magnetic field with Poisson's theorem. Okabe (1979) obtained analytical expressions for the first and second derivative of the gravity potential due to a homogeneous polyhedron with polygonal faces and claimed to sequentially apply twice the divergence theorem. Singh and Guptasarma (2001) computed the gravimetric field due to a polyhedral body with ficticious distribution of mass in points located inside and outside of the body, on planar surface and even on an edge or corner of the body. The same procedure can be applied to calculate the magnetic field from the uniformly magnetic object. The main advantage in their methodology is to compute both fields at the same time, but the article did not show the coding steps. Discretizing the faces in triangles facilitates the understanding of how the magnetic field is generated because the total field produced by the body is just the superposition of the magnetic field of every single triangle. Barros *et al.* (2013) developed a code in MATLAB/OCTAVE language to compute magnetic and gravimetric anomalies of prismatic bodies with arbitrary dimensions showing the application for different bodies. The code is freely distributed.

We have developed analytical expressions for the magnetic anomalies due to a homogeneous polyhedron by adapting and expanding the procedures of Paul (1974) and Werner (1994). In the first step, we applied the divergence theorem to transform the volume integral of the magnetic potentials into surface integrals. The second step consisted of discretizing each face into triangles to obtain the potentials due to each triangle. In the third step, we have employed a coordinate system defined for each triangle ($X_n'$, $Y_n'$, $Z_n'$), instead of the global coordinate system ($X$, $Y$, $Z$). This procedure facilitates the calculation of the integrals, of either of the potentials or of the derived magnetic field components ($B_x$, $B_y$, $B_z$). The derivation and computation of these fields related to the global coordinate system ($X$, $Y$, $Z$) constitutes the last step.

The solution is valid for internal points because the integrals do not diverge at points inside of a mass or a magnetic dipole distribution (Kellogg (2012)). We transformed the double integrals into single integrals solving them analytically or by numerical methods. To validate the procedure, we computed the magnetic anomalies for a rectangular prism and compared with the method presented in Blakely (1996). The maximum error was less than 1.0%.

## THEORY AND METHOD

Each planar face of a homogeneous convex polyhedron was divided into triangles such that the total number of triangles of the solid be $N$. Also, we expressed the magnetic potential, $V(\vec{r})$, due to this polyhedron be an external observation point, $\vec{r} = x\hat{i} + y\hat{j} + z\hat{k}$, of a rectangular system, XYZ, with an origin O as:

$$V(\vec{r}) = C_0 \int_{v_0} \vec{M}(\vec{r_0}) \cdot \nabla_0 \frac{1}{|\vec{r} - \vec{r_0}|} dv_0 \tag{1}$$

In Eq. 1, $C_0 = \frac{\mu_0}{4\pi} = 10^{-7}$ henry meter$^{-1}$ is the magnetic constant, $\mu_0$ representing the permeability of free space, $\vec{M}$ is the magnetization, and $\vec{r}_0 = x_0\hat{i} + y_0\hat{j} + z_0\hat{k}$ is a variable source point inside the polyhedron faces.

Applying the divergence theorem in Eq. 1 we have:

$$V(\vec{r}) = C_0 \sum_{n=1}^{N} \int_{S_{0_n}} \frac{\vec{M}(\vec{r}_0) \cdot \hat{u}_{0_n}}{|\vec{r} - \vec{r}_{0_n}|} dS_{0_n} \tag{2}$$

Therefore, we obtain the magnetic potential as a function of the contributions of the polyhedron's faces. In Eq. 2, $\hat{u}_{0_n}$ is the unit vector perpendicular to each triangular area of every face and its index $n$ refers to each triangle of the faces.

Since these unit vectors will be in different directions, it is necessary to define a local coordinate system, $X_nY_nZ_n$, for each planar face. The systems will have the same origin O; their $Z_n$ axis will be orthogonal and oriented outward of the respective face, and their $X_n$ axis will be parallel to one of the sides of the n-th triangle. The change of coordinates causes a rotation of the axis but no translation. Figure 1 illustrates the scheme.

From the definition of the position of the three vertex, $ABC$, of each triangle,

$$\begin{aligned} \vec{r}_{A_n} &= x_{A_n}\hat{i} + y_{A_n}\hat{j} + z_{A_n}\hat{k}, \\ \vec{r}_{B_n} &= x_{B_n}\hat{i} + y_{B_n}\hat{j} + z_{B_n}\hat{k}, \text{and} \\ \vec{r}_{C_n} &= x_{C_n}\hat{i} + y_{C_n}\hat{j} + z_{C_n}\hat{k}, \end{aligned} \tag{3}$$

we may establish the vectors correspondent to two sides of the triangles: $\vec{AB}_n = \vec{r}_{B_n} - \vec{r}_{A_n}$ and $\vec{AC}_n = \vec{r}_{C_n} - \vec{r}_{A_n}$. Consequently, we determine the unit vectors of the local coordinate systems as:

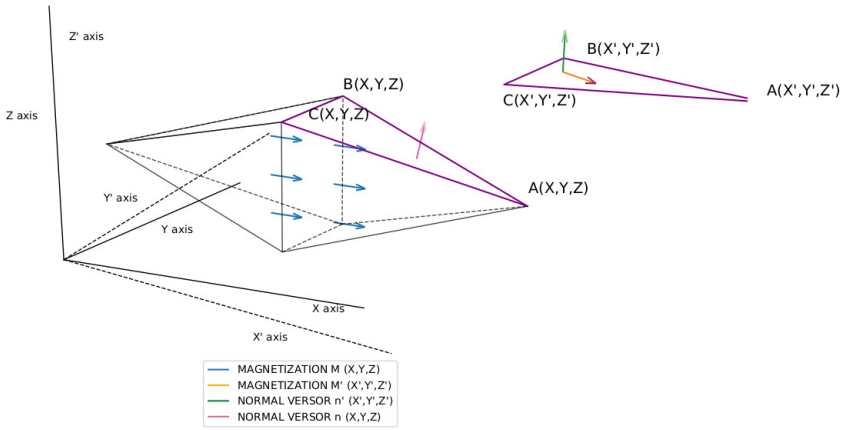


Figure 1. Rotation of the global coordinate system to the coordinate systems of each face.

$$\begin{aligned}\hat{i}' &= \frac{\vec{AB}}{|\vec{AB}|},\\ \hat{k}' &= \frac{\vec{AB}\times\vec{BC}}{|\vec{AB}\times\vec{BC}|},\\ \hat{j}' &= \hat{k}'\times\hat{i}'.\end{aligned} \tag{4}$$

The choice of the vector $\vec{AB}$ has to satisfy the condition that $\hat{k}'$ be oriented outward of the polyhedron. Since all the vectors from the origin remain unchanged in the new coordinate system, we may write:

$$\begin{aligned}\vec{r} &= x'\hat{i}' + y'\hat{j}' + z'\hat{k}',\\ \vec{r}_{A_n} &= x'_{A_n}\hat{i} + y'_{A_n}\hat{j} + z'_{A_n}\hat{k},\\ \vec{r}_{B_n} &= x'_{B_n}\hat{i} + y'_{B_n}\hat{j} + z'_{B_n}\hat{k},\\ \vec{r}_{C_n} &= x'_{C_n}\hat{i} + y'_{C_n}\hat{j} + z'_{C_n}\hat{k},\end{aligned} \tag{5}$$

and the relationship between the components of the vectors in the two coordinate systems is given by:

$$\begin{bmatrix}X'\\ Y'\\ Z'\end{bmatrix} = \begin{bmatrix}\hat{i}\cdot\hat{i}' & \hat{j}\cdot\hat{i}' & \hat{k}\cdot\hat{i}'\\ \hat{i}\cdot\hat{j}' & \hat{j}\cdot\hat{j}' & \hat{k}\cdot\hat{j}'\\ \hat{i}\cdot\hat{k}' & \hat{j}\cdot\hat{k}' & \hat{k}\cdot\hat{k}'\end{bmatrix}\begin{bmatrix}X\\ Y\\ Z\end{bmatrix}. \tag{6}$$

Therefore, we can express the magnetic potentials of a determined triangle of a determined face in its own coordinate system:

$$V(\vec{r}) = C_0\int_{x'_0}\int_{y'_0}\frac{\vec{M'}(\vec{r'}_0)\cdot\hat{k}'}{|\vec{r'}-\vec{r'}_0|}dy'_0dx'_0. \tag{7}$$

The integration limits of $y'_0$ in Equation 7 are a function of $x'_0$. As illustrated in Figure 2, the lower limit is $y'_A = y'_B$ and the upper limits are respectively equal to:

$$\begin{aligned}y_{01}(x') &= y'_A + \frac{(y'_C - y'_A)(x' - x'_A)}{x'_i - x'_A}, \text{ for } x' \le x'_i,\\ y_{02}(x') &= y'_A + \frac{(y'_C - y'_A)(x'_A - x')}{x'_B - x'_i}, \text{ for } x' \ge x'_i.\end{aligned} \tag{8}$$

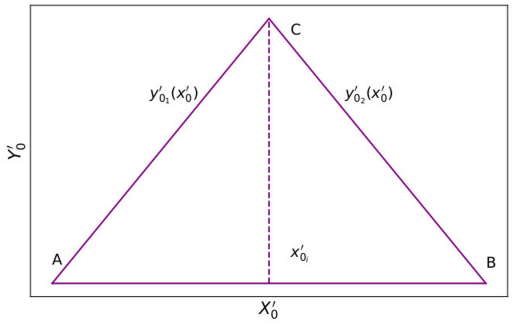


Figure 2. Illustration of the limits of integration in a triangular area.

Under those circumstances the respective components of the magnetic field are given by:

$$
\begin{aligned}
B_x(\vec{r'}) = \; & C_0(\vec{M'}\cdot\hat{k'})(\hat{i'}\cdot\hat{i})\int_{x'_0}\int_{y'_0}\frac{(x'-x'_0)}{|\vec{r'}-\vec{r'_0}|^3}dy'_0dx'_0 + \\
& C_0(\vec{M'}\cdot\hat{k'})(\hat{j'}\cdot\hat{i})\int_{x'_0}\int_{y'_0}\frac{(y'-y'_0)}{|\vec{r'}-\vec{r'_0}|^3}dy'_0dx'_0 + \\
& C_0(\vec{M'}\cdot\hat{k'})(\hat{k'}\cdot\hat{i})(z'-z'_0)\int_{x'_0}\int_{y'_0}\frac{dy'_0dx'_0}{|\vec{r'}-\vec{r'_0}|^3}, \\
B_y(\vec{r'}) = \; & C_0(\vec{M'}\cdot\hat{k'})(\hat{i'}\cdot\hat{j})\int_{x'_0}\int_{y'_0}\frac{(x'-x'_0)}{|\vec{r'}-\vec{r'_0}|^3}dy'_0dx'_0 + \\
& C_0(\vec{M'}\cdot\hat{k'})(\hat{j'}\cdot\hat{j})\int_{x'_0}\int_{y'_0}\frac{(y'-y'_0)}{|\vec{r'}-\vec{r'_0}|^3}dy'_0dx'_0 + \\
& C_0(\vec{M'}\cdot\hat{k'})(\hat{k'}\cdot\hat{j})(z'-z'_0)\int_{x'_0}\int_{y'_0}\frac{dy'_0dx'_0}{|\vec{r'}-\vec{r'_0}|^3}, \\
B_z(\vec{r'}) = \; & C_0(\vec{M'}\cdot\hat{k'})(\hat{i'}\cdot\hat{k})\int_{x'_0}\int_{y'_0}\frac{(x'-x'_0)}{|\vec{r'}-\vec{r'_0}|^3}dy'_0dx'_0 + \\
& C_0(\vec{M'}\cdot\hat{k'})(\hat{j'}\cdot\hat{k})\int_{x'_0}\int_{y'_0}\frac{(y'-y'_0)}{|\vec{r'}-\vec{r'_0}|^3}dy'_0dx'_0 + \\
& C_0(\vec{M'}\cdot\hat{k'})(\hat{k'}\cdot\hat{k})(z'-z'_0)\int_{x'_0}\int_{y'_0}\frac{dy'_0dx'_0}{|\vec{r'}-\vec{r'_0}|^3}.
\end{aligned}
\tag{9}
$$

Adding the contribution of all $N$ triangles yields the magnetic anomalies of the polyhedral body.

Equation 9 can be written as:

$$
B_\eta(\vec{r'}) = \sum_{n=1}^{3}\phi_{\eta n}I_n, \quad \eta = x, y, z. \tag{10}
$$

$\phi_{\eta n}$ is the matrix of the constants. The double integrals $I_1$ and $I_3$ were transformed into single integrals and solved by numerical methods, whereas $I_2$ was solved analytically (see appendix).

The algorithm was written in FORTRAN 90 language to compute the magnetic field from bodies with triangular faces. The triangle parameters were read from an input file. The file has the coordinates of each triangle organized in three columns (X, Y, Z). The points are arranged in a right-handed Cartesian system of coordinates and every triangle has the unitary surface vector pointing out of the polyhedron. The algorithm read them and the magnetic field is computed. It is necessary to discretize the faces of bodies in triangles if the faces are not triangular shaped. An auxiliary code was developed in Python language to prepare the input file for the software which computes the magnetic anomalies in cases where the prismatic bodies have a rectangular base. For other cases, the algorithm needs to be adapted. The output is a text file (.txt) which is compatible with softwares like *Surfer®(Golden Software, LLC)*.

## VALIDATION OF THE METHOD

To validate the method, a cube having 50 m edges and induced magnetization $M = 1$ A/m was positioned with its center at coordinates (100, 100, 50) at the center of a 200 m $\times$ 200 m area. Each face was discretized with four equal triangles performing a total of 24 triangles. We assumed a magnetic inclination of -27° and a magnetic declination of -23°.

The results have been fitted to those computed with the subroutine *mbox* of Blakely (1996).

The error between the fields calculated by our development $(F_{cal})$ and by that subroutine $(F_{sub})$ is given by:

$$
error = 2 \times \frac{|F_{cal} - F_{sub}|}{|F_{cal}| + |F_{sub}|} \times 100\%. \tag{11}
$$

Figure 3 shows the magnetic anomaly due to magnetized cube computed by our method. The relative error is less than 1.0%. Figure 4 shows the behavior of this error on a map. Notice that the maximum values of the error occur for field values close to zero.

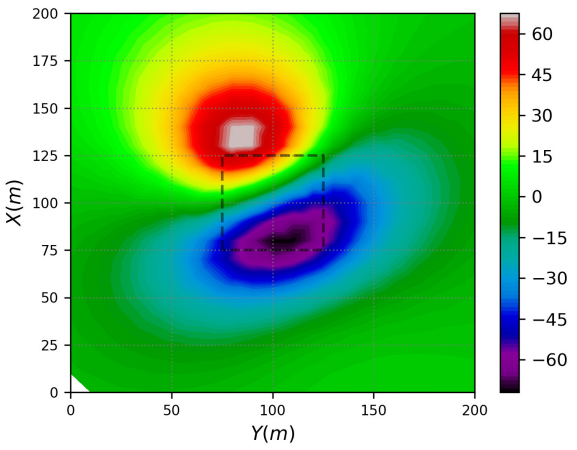


Figure 3. Total field anomaly due to the cube in nT. The dashed line shown is the projection of the cube on the surface indicating where the cube is located on the map.

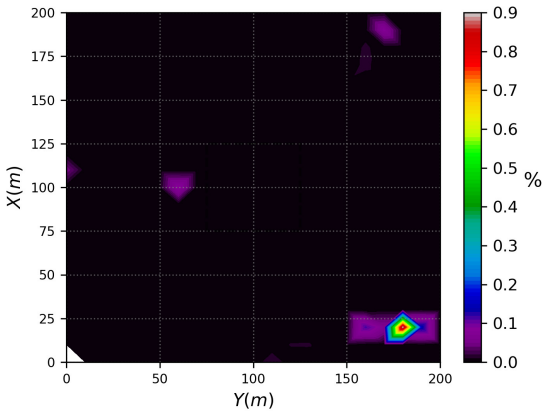


Figure 4. Map of the relative error between the two methods.

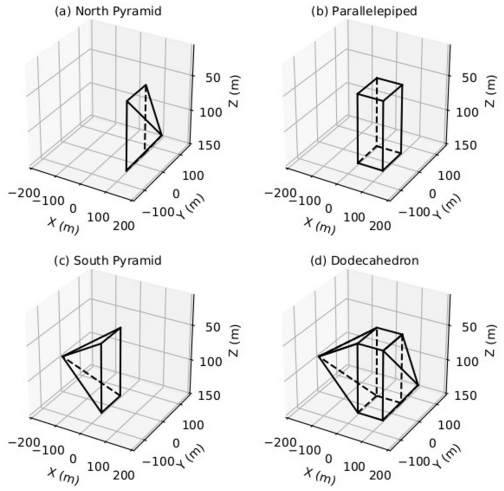


Figure 5. Configuration of the four polyhedrons used to compute the magnetic anomalies displayed, respectively, in Figure 6.

## RESULTS

The inducing field for the cases analysed here has an inclination of -27° and a declinaton of -23°. By decomposing it along two directions: one parallel and the other perpendicular to each face, only the perpendicular component will magnetize the face by induction. The magnetic field of each body results from the contribution of its faces and the contribution of each face depends on its size and spatial orientation. Therefore, given equal sizes, a face with the smallest angle between its normal versor and the inductive field direction contributes more than a face with a different planar orientation.

Figure 5 presents the configuration and the coordinates of four polyhedrons: two pyramids, one parallelepiped and one dodecahedron. The angle $\theta$ between the perpendicular component of the inducing field and the outward normal versor of a face may assume two values: $\theta = 0°$ for an outward field and $\theta = 180°$ for an inward field relative to the face. The first case produces a secondary field congruent with the inductive field and the second case produces a secondary field opposing the inductive field. Three faces of the northern pyramid are congruent and two are opposed, three faces of the southern pyramid are opposed and two are congruent, three faces of the parallelepiped are opposed and three are congruent.

Figure 6 shows the magnetic anomalies due to the solids of Figure 5. Taking as a reference the field produced by the parallelepiped, notice that the line joining the nuclei of the anomalies due to the two pyramids are displaced in the east-west direction. This fact results from the geometry of the bodies and of the orientation and inclination of their faces relative to the inducing field. The field produced by the dodecahedron is the sum of the other three.

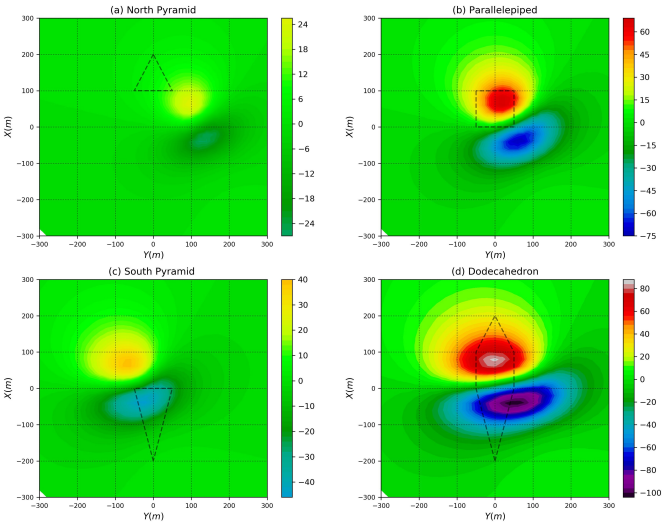


Figure 6. Magnetic anomalies (nT) of the four polyhedrons shown in Figure 5 magnetized by an inducting field with inclination of -27° and declination of -23°. The dashed lines shown are the projections of bodies on the surface and they indicate where the bodies are located on the map.

Figure 7 presents the configuration and the coordinates of the vertices of four octahedrons and Figure 8 displays their respective magnetic anomalies. The third and the fourth octahedrons have the same shape as the first but are inclined 25° north and south, respectively. The second has the same orientation of the first but has an irregular shape. The dashed lines in Figure 8 indicate their projection on the plane $Z = 0$ m. For the third

and fourth solids, the semi-axis along the $X$ direction with a shorter size indicate the direction of the dip.

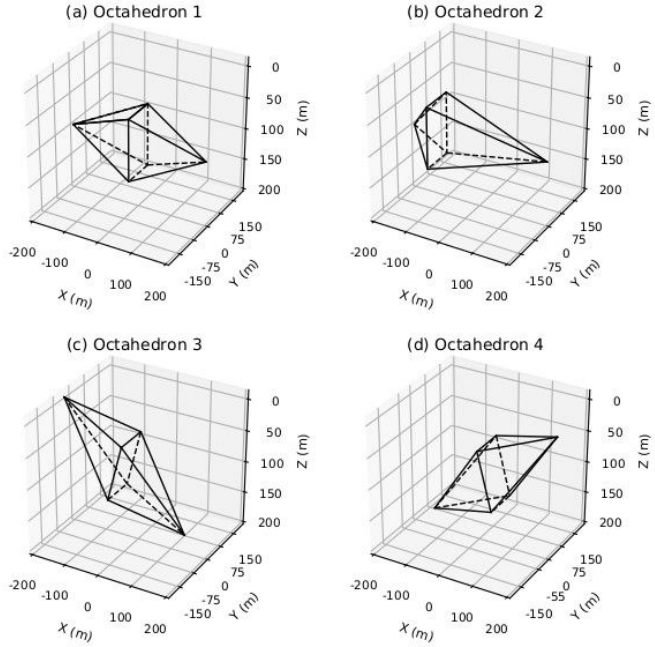


Figure 7. Configuration of the four octahedrons used to compute the magnetic anomalies displayed respectively, in Figure 8.

Due to the orientation of the inducing field, the southeastern, the upper southern, the northwestern, and the lower northern faces contribute more for the magnetic anomaly than the other four; the first two are opposed and the last two are congruent to the inducing field. So, the positions of the nuclei of the magnetic anomalies depend on their sizes and orientations.

Octahedron 1 is symmetric with respect to the three coordinate axes (plane $Z = 100\,\text{m}$) and its anomaly nucleus are close to $Y = 0\,\text{m}$. The non-symmetric condition of octahedron 2 with respect to the $X$ axis, produces a western displacement of those nuclei. Octaehdrons 3 and 4 are identical to the first body and produce similarly shaped anomalies, but as mirrored images around $Y = 0\,\text{m}$. However, there is a change in amplitude of the magnetic field. The east-west deviation occurs because of the dip. This shows that, in regions of the southern hemisphere with western declination, a northerly dipping body deviates the magnetic anomaly to the west and a southerly dipping body deviates it to the east.

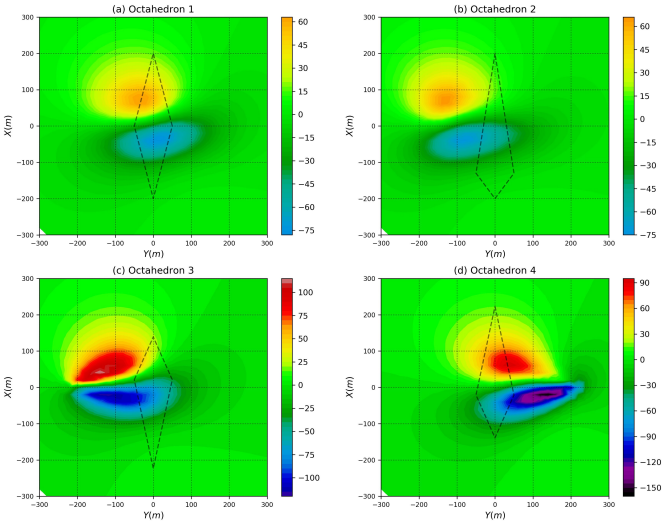


Figure 8. Magnetic anomalies (nT) of the four octahedrons shown in Figure 7 magnetized by an inducting field with inclination of -27° and declination of -23°. The dashed lines shown are the projections of bodies on the surface and they indicate where the bodies are located on the map.

## CONCLUSION

This new approach will be useful for the inverse modeling and interpretation of magnetic anomalies of complex shaped bodies, especially in mining exploration, since mineralized bodies have shapes very different from those commonly used: prisms, spheres and cylinders.

The misfit smaller than 1.0% between this procedure and the closed form for prismatic bodies shows that we may decrease computer costs avoiding the discretization of too many triangles. The present development is not restricted to the determination of the anomalies at external observation points of homogeneous regular convex polyhedrons. It may be adapted to inhomogeneous solids by modeling them as constituted of several smaller homogeneous bodies. It may also determine values at internal observation points, in order to simulate data collected along drill holes and mine shafts.

## ACKNOWLEDGMENTS

Amarante acknowledges the fellowships from CAPES and E. Sampaio acknowledges the fellowship from CNPq.

## APPENDIX

Integrals $I_2$ have four possible solutions: (1) for $C_k > 0$ and $\Delta_k < 0$; (2) for $C_k > 0$ and $\Delta_k = 0$; (3) for $C_k > 0$ and $\Delta_k > 0$; and (4) for $C_k < 0$ and $\Delta_k < 0$, where $\Delta = 4A_kC_k - B_k^2$. The coefficients $A_k$, $B_k$, and $C_k$ are given as functions of the geometrical parameters of the triangles – the angular and linear coefficients of the straight lines joining the vertex $a_k$ and $b_k$ and the observation stations $x'$, $y'$ and $z'$. Consequently, $A_k = x'^2 + y'^2 + (z' - z'_0)^2 - 2y'b_k + b_k^2$, $B_k = -2x' - 2y'a_k + 2a_kb_k$, and $C_k = 1 + a_k^2$.

### First solution

$$I_{l2}(\vec{r'}) = \ln\Big[\Big(\frac{P_{22}}{P_{21}}\Big)^{\frac{1}{\sqrt{C_2}}}\Big(\frac{P_{11}}{P_{12}}\Big)^{\frac{1}{\sqrt{C_1}}}\Big], \qquad (12)$$

$P_{kj} = 2C_k\sqrt{C_kR_{kj}} + 2C_kx'_{0_j} + B_k$, and $R_{kj} = A_k + B_kx_j + C_kx_j^2$.

### Second solution

$$I_{l2}(\vec{r'}) = \ln\Big[\Big(\frac{W_{22}}{W_{21}}\Big)^{\frac{1}{\sqrt{C_2}}}\Big(\frac{W_{11}}{w_{12}}\Big)^{\frac{1}{\sqrt{C_1}}}\Big], \qquad (13)$$

$W_{kj} = 2C_kx'_{0_j} + B_k$.

### Third solution

$$I_{l2}(\vec{r'}) = \frac{1}{i\sqrt{C_2}}\Big[\arcsin\Big(\frac{iW_{22}}{\sqrt{\Delta_2}}\Big) - \arcsin\Big(\frac{iW_{21}}{\sqrt{\Delta_2}}\Big)\Big] - \frac{1}{i\sqrt{C_1}}\Big[\arcsin\Big(\frac{iW_{12}}{\sqrt{\Delta_1}}\Big) - \arcsin\Big(\frac{iW_{11}}{\sqrt{\Delta_1}}\Big)\Big] \qquad (14)$$

### Fourth solution

$$I_{l2}(\vec{r'}) = \frac{-1}{\sqrt{-C_2}}\Big[\arcsin\Big(\frac{W_{22}}{\sqrt{-\Delta_2}}\Big) - \arcsin\Big(\frac{W_{21}}{\sqrt{-\Delta_2}}\Big)\Big] + \frac{1}{\sqrt{-C_1}}\Big[\arcsin\Big(\frac{W_{12}}{\sqrt{-\Delta_1}}\Big) - \arcsin\Big(\frac{W_{11}}{\sqrt{-\Delta_1}}\Big)\Big] \qquad (15)$$

**E.M.S.A.:** Algebra development (lead), modelling, methodology (equal), coding, data analysis (lead) and writing (lead). **E.E.S.S.:** Algebra development (supporting), methodology (equal), data analysis (supporting) and writing (supporting).

## REFERENCES


Barros, A.; Bongiolo, S.; de Souza, J.; Ferreira, F.J.F.; de Castro, L.G. GRAV MAG PRISM: a matlab/octave program to generate gravity and magnetic anomalies due to rectangular prismatic bodies. *Brazilian Journal of Geophysics* **2013**, *31*, 347–363.

Blakely, R.J. *Potential theory in gravity and magnetic applications*; Cambridge University Press, 464p, 1996.

Cady, J.W. Calculation of gravity and magnetic anomalies of finite-length right polygonal prisms. *Geophysics* **1980**, *45*, 1507–1512.

Götze, H.J.; Lahmeyer, B. Application of three-dimensional interactive modeling in gravity and magnetics. *Geophysics* **1988**, *53*, 1096–1108.

Kellogg, O.D. *Foundations of potential theory*; Vol. 31, Springer Science & Business Media, 393 p, 2012; p. 393.

Okabe, M. Analytical expressions for gravity anomalies due to homogeneous polyhedral bodies and translations into magnetic anomalies. *Geophysics* **1979**, *44*, 730–741.

Paul, M. The gravity effect of a homogeneous polyhedron for three-dimensional interpretation. *Pure and Applied Geophysics* **1974**, *112*, 553–561.

Singh, B.; Guptasarma, D. New method for fast computation of gravity and magnetic anomalies from arbitrary polyhedra. *Geophysics* **2001**, *66*, 521–526.

Werner, R.A.; Scheeres, D.J. Exterior gravitation of a polyhedron derived and compared with harmonic and mascon gravitation representations of asteroid 4769 Castalia. *Celestial Mechanics and Dynamical Astronomy* **1996**, *65*, 313–344.

Werner, R.A. The gravitational potential of a homogeneous polyhedron or don't cut corners. *Celestial Mechanics and Dynamical Astronomy* **1994**, *59*, 253–278.


Received on August 24,2020/ Accepted em April 28, 2021.